BOLETIN DE LA SOCIEDAD ESPAÑOLA DE
Cerámica y Vidrio
www.elsevier.es/bsecv

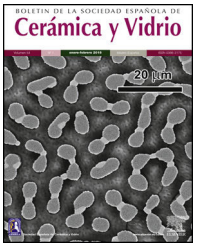

Original

Microstructure and mechanical properties of 4YTZP-SiC composites obtained through colloidal processing and Spark Plasma Sintering

Amparo Borrell[a,*], *Lucia Navarro*[a], *Carlos F. Gutiérrez-González*[b], *Carmen Alcázar*[c], *María D. Salvador*[a], *Rodrigo Moreno*[c]

[a] *Instituto de Tecnología de Materiales, Universitat Politècnica de València, Camino de Vera s/n, 46022 Valencia, Spain*
[b] *Nanoker Research S.L., Polígono Industrial Olloniego, Parcela 22A, nave 5, 33660 Oviedo, Spain*
[c] *Instituto de Cerámica y Vidrio (ICV), Consejo Superior de Investigaciones Científicas (CSIC), Kelsen 5, E-28049 Madrid, Spain*

ARTICLE INFO

Article history:
Received 3 September 2019
Accepted 31 January 2020
Available online 20 February 2020

Keywords:
Zirconia
Silicon carbide
Spark plasma sintering
Mechanical properties
Microstructure

ABSTRACT

Bulk composites of silicon carbide reinforced zirconia were obtained through colloidal processing and spark plasma sintering, and their microstructural and mechanical properties were investigated. Mixtures of powders of 4 mol% yttria-doped zirconia and silicon carbide, with percentages of 15 and 20 wt% of silicon carbide, were prepared by colloidal processing and freeze-drying to guarantee the homogeneity of powders, and sintered by SPS at temperatures ranging from 1300 to 1400 °C to obtain dense composites. The spark plasma sintering technique makes it possible to control sintering energy and speed, and impedes the oxidation of silicon carbide to ensure larger reproducibility. The microstructure of the composites reveals that some defects arise during sintering due to the differences of coefficient of thermal expansion between zirconia and silicon carbide. Mechanical properties were studied, such as Vickers hardness, Young's modulus, and bending strength. Compared with 4YTZP monolithic material, composites have better fracture strength values (~588 MPa and 492 MPa, for 15 wt% and 20 wt% of silicon carbide, respectively) when sintered at 1400 °C. It is also demonstrated that silicon carbide particles act as an absorption centre for propagating cracks.

Microestructura y propiedades mecánicas de composites 4YTZP-SiC obtenidos por procesamiento coloidal y Spark Plasma Sintering

Palabras clave:
Circona
Carburo de silicio

RESUMEN

En este estudio se investigaron las propiedades microestructurales y mecánicas de los composites de circona reforzados con carburo de silicio (SiC) obtenidos mediante procesamiento coloidal y sinterización por descarga eléctrica (*spark plasma sintering* [SPS]). Se prepararon

* *Corresponding author.*
E-mail address: aborrell@upv.es (A. Borrell).
https://doi.org/10.1016/j.bsecv.2020.01.014

Spark plasma sintering
Propiedades mecánicas
Microestructura

mezclas de circona dopada con 4 %mol de itria (4YTZP) y SiC con porcentajes del 15 y 20% en peso mediante procesamiento coloidal y liofilización para garantizar la homogeneidad de los polvos, posteriormente se sinterizaron por SPS a temperaturas de 1300 a 1400 °C para obtener composites densos. La técnica de SPS permite controlar el tiempo y la velocidad de sinterización e impide la oxidación del SiC para garantizar una mayor reproducibilidad. La microestructura de los composites ha revelado algunos defectos durante la sinterización debido a las diferencias de coeficiente de expansión térmica entre la 4YTZP y el SiC. Por otro lado, se estudiaron las propiedades mecánicas como la dureza Vickers, el módulo de Young y la resistencia a la flexión. En comparación con el material monolítico de 4YTZP sinterizado a 1400 °C, los composites presentan mejores valores de resistencia a la fractura (∼ 588 MPa y ∼ 492 MPa, con un 15 y un 20% en peso de SiC, respectivamente). También se ha demostrado que las partículas de SiC actúan como centro de absorción de propagación de grietas.

Introduction

Yttria-doped polycrystalline tetragonal zirconia (YTZP) is an interesting material for many structural applications due to its excellent properties at high temperatures compared to metals, its high strength accompanied by high toughness, low thermal expansion coefficient, great thermal stability and chemical resistance. However, YTZP is not a tough material, and its mechanical properties must be increased to extend its applications [1]. One feature that has been investigated in recent years is the combination of YTZP and SiC to obtain new functionality materials [2].

SiC has been the most popular non-oxidic ceramic material in the industry for more than a century. Due to its electrical and mechanical properties at high temperatures, it is widely used as a structural component [3]. Dispersed SiC particles in a YTZP matrix can produce ceramic composites with enhanced mechanical properties due to their excellent thermal shock resistance and oxidation resistance despite their poor sinterability and low fracture toughness [4]. It is also known that SiC has an important crack-healing ability [5,6]. YTZP/SiC composites have been widely studied by Bamba et al. [7–9], who determined that SiC particles in a YTZP matrix enhance the fracture strength from 300 MPa to 750 MPa using 20 vol.% of SiC, favouring crack deflection when the composite is sintered by hot pressing. Hong et al. [10] studied YTZP/SiC composites, demonstrating that the dispersion of SiC in a YTZP matrix slightly increases its mechanical properties.

In order to obtain better reproducibility and results of YTZP/SiC ceramic composites, it is important to control the physicochemical parameters with the aim of reducing defects in the sintered materials. This can be achieved by improving the homogeneity of powders and reducing the presence of agglomerates which, in turn, can be done by controlling the intimate mixing of the components through colloidal processing. There are a lot of factors that determine the success of colloidal processing, such as powder size distribution and the shape, surface properties and interaction forces between particles and solvents [11]. Measuring the zeta potential and optimising the rheological behaviour makes it possible to determine the optimum conditions for the efficient dispersion of powders and the preparation of suspensions with higher solid contents to achieve better packing densities.

On the other hand, the development of cutting-edge sintering technology is associated with the need to fabricate new materials with multifunctional properties. SPS is a non-conventional technique that can very quickly sinter ceramic powders and produce fully dense compacts [12]. This technique can work at heating rates of the order of one hundred degrees per minute combined with external pressure assistance, reaching high temperatures in a very short space of time [13]. Hence, ceramic composites sintered by SPS show high mechanical properties while maintaining small grain sizes, as there is no time for coarsening [14].

This sintering technique is being profusely applied in the preparation of a wide range of materials, but only a few scientific publications can be found on the topic of SPS-sintered ZrO_2/SiC composites [15,16]. Nevertheless, to the best of our knowledge, no data is available on the influence of the rheological behaviour of the starting powders and SPS parameters on the performance and microstructure of these materials.

The main objective of this work was to obtain homogeneous zirconia/silicon carbide (4YTZP/SiC) powder mixtures by colloidal processing and subsequent spark plasma sintering at relatively low temperatures (1300–1400 °C). For this purpose, submicron-sized 4YTZP and SiC powders were well dispersed in water, freeze-dried and subsequently sintered to obtain dense composites. The resulting materials were evaluated in terms of their microstructure and mechanical properties. The results were compared with a 4YTZP monolithic material prepared under the same conditions.

Materials and methods

Commercial powder of tetragonal zirconia polycrystals doped with 4 mol% Y_2O_3 (TZ4YS, Tosoh, Japan) and α-SiC (UF-15, Hermann C. Stark, Germany) were used as starting powders. Starting zirconia powder has a theoretical density of 6.05 g/cm^3, an average particle size of 0.7 μm and a surface area of powder is 7.0 m^2/g according to the provider's data. α-SiC powder has a theoretical density of 3.21 g/cm^3, an average particle size of 0.6 μm and a surface area of 15 m^2/g

according to the provider's data. Particle size distributions were measured using the laser diffraction technique (LD, Mastersizer S, Malvern, UK), and the surface area was measured using the N_2-adsorption BET method with a Monosorb Surface Area Analyser MS-13 (Quantachrome Co., USA). The morphology and microstructure of the as-received powders were observed after sintering using field emission-scanning electron microscopy (FE-SEM, Gemini Ultra 55 model, Zeiss).

The colloidal stability was studied by measuring the zeta potential of the starting powders as a function of pH with and without polyelectrolytes, in order to determine the optimum amount of dispersant and the most effective pH operation conditions. The measurements were performed through a laser Doppler principle combined with non-invasive back-scattering equipment (Zetasizer Nano-ZS, Malvern, UK). Aqueous suspensions with a solid content of 0.1 g L^{-1} were prepared by using KCl 10^{-2} M as inert electrolyte and adjusting the pH values using KOH and HCl 10^{-1} M solutions. These adjustments were made with a pH-metre (Titrino DMS 716, Metrohm, Switzerland). In order to prevent agglomerates that might interfere with the results, a sonication probe (UP 400S, Dr Hielscher GmbH, Germany) was used at a frequency of 24 kHz for 1 min. The suspension was also immersed in an ice bath during sonication to prevent overheating. As regards deflocculants, a poly(acrylic acid)-based polyelectrolyte (Duramax TM D3005, Rohm & Haas, USA, with 35 wt% active matter) was used for 4YTZP, and a synthetic polyelectrolyte (Produkt KV5088, Zschimmer-Schwarz, Germany), which has demonstrated its suitability for the dispersion of non-oxide ceramics, was used to disperse the SiC powders [17].

In order to maximise the concentration in solids of the suspension while maintaining low viscosity values, suspensions with solid contents from 10 to 40 vol.% were prepared. These suspensions were always prepared through the same procedure, maintaining water with the desired content of deflocculant by continuous mechanical agitation with helices and then slowly adding the 4YTZP powders. For the suspensions combining 4YTZP and SiC, PKV was added to a previous 4YTZP aqueous suspension, and then SiC powders were incorporated while maintaining the mechanical agitation. Prepared compositions included bare 4YTZP and with 15 and 20 wt% SiC (compositions labelled as 4YTZP, 15SiC, and 20SiC, respectively).

The rheological characterisation of the prepared suspensions was carried out using a rotational rheometer (MARS, Thermo Haake, Germany) with double-cone/plate sensor configuration with a cone angle of 2° equipped with a solvent trap to prevent evaporation (DC60/2, Thermo Haake, Germany). The temperature was kept constant at 25 °C by means of a temperature water bath controller. The measuring programme was carried out under controlled shear rate mode using a three-stage measuring cycle. The first stage was the linear increase of the shear rate from 0 to 1000 s^{-1} in 5 min, followed by a plateau at the maximum shear rate (1000 s^{-1}) for 1 min, and the third stage was a decrease in the shear rate from 1000 to 0 s^{-1} in 5 min. Sonication was performed using several 1-min cycles with a maximum sonication of 3 min, since further sonication cycles would lead to agglomeration.

After selecting the optimal conditions to obtain a stable and homogeneous suspension, the materials were placed in volumetric flasks, which were coupled to a rotary evaporator (120 rpm, RV10 basic, IKA, Germany) and frozen using a liquid N_2 bath. Afterwards, frozen suspensions were freeze-dried (Cryodos 50, Telstar, Spain) to sublimate the water present in the frozen material at a pressure of 5 Pa and a condenser temperature of −50 °C for 24 h. The obtained powders were sieved through a 63 μm mesh. The composite powders were also dispersed in aqueous suspensions that were subsequently freeze-dried following the same methodology.

The resulting dry powders were placed in a graphite die with an inner diameter of 20 mm and cold uniaxially pressed at 30 MPa. Then they were placed in spark plasma sintering apparatus HP D25/1 (FCT Systeme GmbH, Rauenstein, Germany) under low vacuum (1 Pa) and sintering temperatures from 1300 to 1400 °C, and a constant and uniaxial compaction pressure of 80 MPa was applied from the beginning of the sintering cycle. Tests were carried out with a heating rate of 100 °C min^{-1} and 5 min of dwelling time at maximum temperature.

The Archimedes method was used to measure the sintered density in line with the ASTM-C-373 standard [18]. XRD patterns of powder and crystalline bulk materials were collected and mounted in appropriate sample holders (XRD, D8 Advance, Bruker, Germany). Patterns were collected with a scanning step of 0.02° between 20 and 70° in 2θ.

The mechanical properties were determined on surfaces that had been polished down to 0.25 μm particle size with diamond paste using a Struers polisher model Labopol-5 (USA). The fracture strength was measured using biaxial testing (ASTM F394-78), by using equations proposed by Kirstein and Woollen [19] and Vitman and Pukh [20].

$$\sigma_F = \frac{3 \cdot F \cdot (1+\upsilon)}{4 \cdot \pi \cdot t^2} \cdot \left[1 + 2\ln\frac{R_a}{b} + \frac{(1-\upsilon)}{(1+\upsilon)} \cdot \left(1 - \frac{b^2}{2 \cdot {R_a}^2}\right) \cdot \frac{{R_a}^2}{R^2}\right] \quad (1)$$

where F is the maximum load before breaking the sample, t is the thickness of the specimen, R_a is the radius of the circle formed by the balls that bear the specimen, b is a geometric approach [21], υ is the Poisson ratio of the specimen and R is the radius of the specimen. All the samples analysed have a diameter of 20 mm and a thickness of 3 mm, the preparation for mechanical tests consist in polishing one side after ensuring that the two sides of the disc for biaxial flexural test are planoparallel. All tests were conducted at room temperature using a universal testing machine (Shimadzu AG-X Plus, Japan) with a span length of 12 mm and a cross-head displacement of 0.002 mm/s. Five samples were testing for each temperature.

Vickers hardness (H_V) measurements were made with a Vickers tester (Shimadzu HMV-20); H_V tests were performed by applying a load of 3 N for 10 s; 10 measurements were taken for each sample.

Young's modulus, E, was evaluated using the nanoindentation technique. This consists of a nanoindenter equip (Model G-200, MTS Company, USA) with a Berkovich diamond tip previously calibrated with silica standard. Tests were performed under a maximum depth control of 1300 nm. The continuous stiffness measurement technique was used to determine the contact stiffness (S) and calculate the profiles

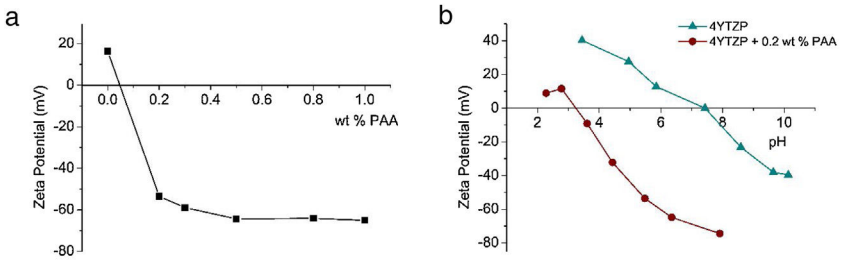

Fig. 1 – Evolution of zeta potential of 4YTZP diluted suspensions (a) as a function of PAA concentration at pH = 9 and (b) without and with 0.2 wt% content of PAA as a function of pH.

of E. A matrix with 9 indentations was evaluated for each sample.

Results and discussion

Fig. 1 presents the results of the stability studies for 4YTZP suspensions using zeta potential measurements. Fig. 1a shows the variation of zeta potential with the deflocculant concentration for 4YTZP diluted suspensions using PAA as a deflocculant at their natural pH (around pH = 9). As expected from other studies using a similar powder with 3 mol% Y_2O_3, the surface charge of 4YTZP particles changes abruptly from positive to negative with small PAA additions [22]. PAA is absorbed into the surface of the particles even with only 0.2 wt% addition, a concentration high enough to induce a highly negative zeta potential (−57 mV) to ensure a high stability at the working pH, between 8 and 9. Therefore, 0.2 wt% PAA content was selected as an appropriate quantity to prepare concentrated, stable suspensions. To confirm this choice, further studies were carried out on the zeta potential dependence versus the pH of 4YTZP diluted suspensions with and without the addition of 0.2 wt% PAA. The results are presented in Fig. 1b. As predicted, the addition of anionic polyelectrolyte strongly shifts down the isoelectric point from around pH 7 for the 4YTZP suspension without deflocculant to ~3.2 with 0.2 wt% PAA. High absolute values of zeta potential indicate high stability; these results suggest that it is possible to prepare a stable suspension at pH ~ 9 using 0.2 wt% PAA. These values match the previously reported data for 3YTZP [22,23], in which a similar shift down from pH 6 to values slightly higher than pH 3 was reported.

SiC stability had already been studied in previous works. *Candelario et al.*[17] showed that the isoelectric point of SiC occurred at pH 3.8 and demonstrated that a dispersant content of 1.5 wt% of PKV was the best choice to achieve maximum stability with zeta potential absolute values higher than 30 mV at pH ≥ 6. These studies also concluded that PKV did not significantly change the isoelectric point, but allowed the preparation of concentrated suspensions with low viscosity due to its steric effect.

In this work, once the dispersing conditions had been selected, concentrated suspensions of 4YTZP were prepared with and without the secondary SiC phase. The rheological behaviour of the 4YTZP suspensions was the first aspect to be studied. Concentrated suspensions were prepared in deionised water to a solid loading of 30 vol.% at their natural pH (i.e. 9) using different deflocculant contents, from 0.1 to 0.5 wt%, and different sonication times. Fig. 2 shows the flow curves of 30 vol.% 4YTZP suspensions with 0.2 wt% PAA varying the sonication time. It may be observed that the best sonication time is 2 min, and longer ultrasound treatments lead to a small re-agglomeration, since the suspension viscosity increases. Fig. 3 presents the flow curves of suspensions dispersed with different contents of PAA and sonicated for 2 min, showing that the lowest viscosity is obtained for a PAA content of 0.2 wt%, thus confirming the results predicted from the zeta potential measurements. Suspensions with 0.1 wt% PAA have

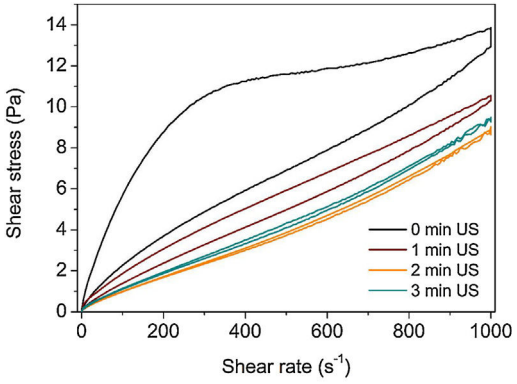

Fig. 2 – Flow curves of 30 vol.% solids content 4YTZP suspensions with 0.2 wt% of deflocculant varying sonication time.

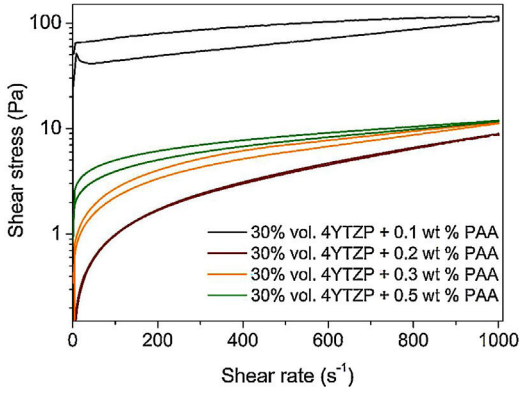

Fig. 3 – Flow curves of concentrated 4YTZP suspensions with 0.1–0.5 wt% deflocculant content and with optimum sonication time (2 min).

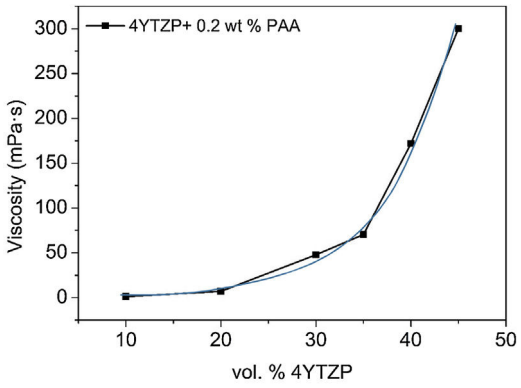

Fig. 4 – Viscosity of 4YTZP suspensions dispersed with 0.2 wt% PAA and 2 min sonication as a function of solids loading.

a high viscosity and very broad thixotropic cycle, demonstrating their lack of stability. The increase of dispersant content to 0.2 wt% decreases the viscosity, and the curve does not present thixotropy, which indicates good homogeneity. Further additions of PAA lead to slightly higher viscosities. Accordingly, high concentrated suspensions with solid contents ranging from 10 to 40 vol.% were prepared using 0.2 wt% of PAA.

Fig. 4 represents the high shear viscosity (1000 s^{-1}) of suspensions of 4YTZP containing different solid loadings. This plot shows that suspensions maintain very low viscosity and good flowability up to a solid content of 35 vol.% and, from 40 vol.%, viscosity is relatively high and flowability is poor. The relationship between viscosity and solid loading is exponential, as was expected in accordance with the literature [11].

Once the rheological behaviour of 4YTZP suspensions with a high solid content had been studied and the optimum dispersing conditions had been determined, 30 vol.% suspensions of the mixtures 4YTZP/SiC were prepared using 0.2 wt% PAA to disperse 4YTZP and 1.5 wt% PKV to disperse SiC. Fig. 5 shows the flow curves of both 4YTZP/SiC suspensions containing 15 wt% of SiC (Fig. 5a) and 20 wt% SiC (Fig. 5b). As illustrated by these figures, suspensions without sonication are not effectively dispersed and present very broad thixotropic cycles, whereas those sonicated for 1 min present the best rheological behaviour of each series with nearly Newtonian behaviour and no thixotropy. In addition, the composite suspensions have a similar viscosity which, in turn, is similar to the 4YTZP suspension, as shown in Fig. 2. The 4YTZP/SiC suspensions were well stabilised, as both have negative charges at pH 9, thus ensuring an effective electrostatic contribution to the stabilisation to prevent the natural tendency from forming aggregates induced by London-Van der Waals forces [24,25]. Despite the negligible thixotropy, viscosity values at 1000 s^{-1} are 10.5 MPa s to 4YTZP, 7.5 MPa s to 30 vol.% suspensions of 4YTZP/15SiC and 7.9 MPa s to 30 vol.% suspensions of 4YTZP/20SiC.

The optimised suspensions were freeze-dried, and the resulting powders were sintered by SPS at 1300, 1350 and 1400 °C. Fig. 6 compares the X-ray diffraction patterns of 15SiC and 20SiC freeze- dried powders and after sintering by SPS at 1400 °C.

X-ray analysis reveals that freeze-dried powders consisted of zirconia with tetragonal as the major phase, as well as a small contribution of monoclinic phase and SiC.

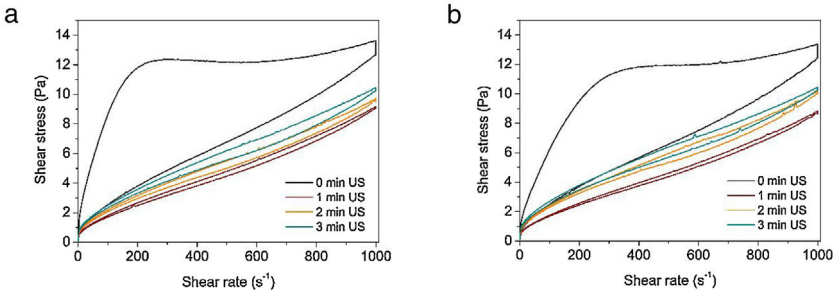

Fig. 5 – Flow curves of concentrated suspensions of 4YTZP/SiC dispersed using 0.2 wt% PAA for 4YTZP and 1.5 wt% PKV for SiC, prepared to 30 vol.% solids content with and without different sonication times: (a) 15 wt% SiC and (b) 20 wt% SiC.

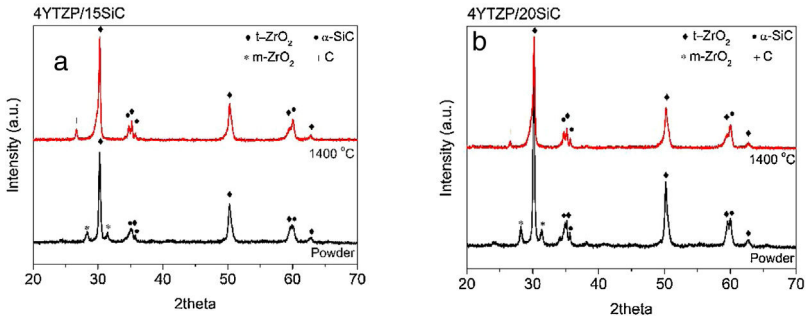

Fig. 6 – X-ray diffraction patterns of 4YTZP/SiC freeze-dried powders and bulk-materials after-sintering at 1400 °C by SPS: (a) 15 wt% SiC and (b) 20 wt% SiC.

Table 1 – Relative densities (experimental values, g/cm^3, and % TD) of sintered materials by SPS at 1300, 1350, and 1400 °C.

	Sintering temperature (°C)					
	1300		1350		1400	
4YTZP	6.04 g/cm^3	99.8%	6.04 g/cm^3	99.9%	6.04 g/cm^3	99.9%
15SiC	5.39 g/cm^3	95.8%	5.37 g/cm^3	95.5%	5.38 g/cm^3	95.7%
20SiC	5.25 g/cm^3	95.7%	5.24 g/cm^3	95.5%	5.24 g/cm^3	95.6%

After sintering, X-ray shows a peak of carbon due to the graphite die used during the SPS process. During the sintering cycle, all the monoclinic phase of ZrO_2 transformed into the tetragonal phase and no reaction phase was detected. The use of graphite die during sintering promotes a reductive atmosphere to prevent the reaction of ZrO_2 and SiC [9].

The relative density of sintered materials as a function of final temperature is shown in Table 1. Almost theoretical density (≥99.8% relative density) was obtained for 4YTZP monolithic materials sintered at any temperature in the range considered. The relative density of 4YTZP/SiC composites exceeds >95% but does not approach the theoretical density. However, the final density of the composites is similar for all sintering temperatures.

The incorporation of SiC particles as a secondary phase reduces densification at low temperatures, and it is widely known that the full densification of SiC ceramics is especially complicated without sintering additives, mainly due to the covalent nature of the silicon carbide bond, which in the sintering process shows very low diffusivity of atoms and high energy on the grain boundaries [26]. In this work, 4YTZP/SiC composites were sintered without adding any specific sintering aid. It is known that SiC powders need high temperature to reach full densification, but in this work the matrix is zirconia, and a sintering temperature higher than the one selected here could lead to exaggerated grain growth and transformation of zirconia to cubic phase. This would lead to expansion until cracking, causing a decrease of its mechanical properties and limiting its structural applications.

FE-SEM micrographs of the fracture surfaces of 4YTZP and 4YTZP/SiC composites obtained by SPS at 1300 °C are shown in Fig. 7. It is important to note that the monolithic 4YTZP material reaches full densification without residual porosity, as observed in Fig. 7a. On the contrary, the incomplete densification of the composites can be clearly observed regardless of the SiC percentage. Although the final density was similar for the two composites, there were differences in the final microstructure, as shown in Fig. 7b and c. The 4YTZP material achieves its maximum density values due to the fact that all grains are close to their maximum compaction with small zirconia grains homogeneously dispersed without agglomerates (Fig. 7a). 4YTZP/SiC composites show some coarsening of both 4YTZP and SiC grains as the SiC percentage increases. SiC particles are not integrated in the matrix, as revealed by the micrographs in Fig. 7b and c. The sample with 20 wt% of SiC presented the inhomogeneous dispersion of SiC particles in a ZrO_2 matrix, leading to submicrometric large pores and SiC grains of >1 μm.

The Vickers hardness, Young's modulus and fracture strength of the materials fabricated by SPS are shown in Fig. 8 as a function of the final sintering temperature.

The Vickers hardness values increase with the final sintering temperature. All composites obtained by SPS at different temperatures show values lower than that of the zirconia material (15.4 GPa at 1400 °C). Another direct observation is that when the percentage of SiC increases, the hardness values decrease. Two main factors affect the hardness values of these composites: the low density values of the materials; and the increase in grain growth, which is proportional to the concentration of SiC particles. This is associated with the presence of porosity on the one hand, and the increasing average grain size leading to a decrease in hardness on the

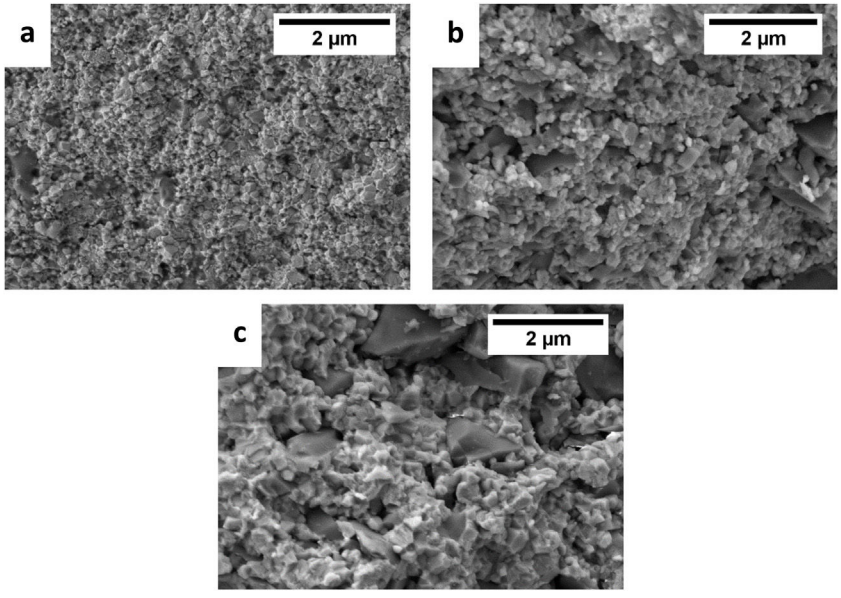

Fig. 7 – FE-SEM micrographs of fracture surfaces: (a) 4YTZP material and composites, (b) 15 wt% SiC and (c) 20 wt% SiC, sintered by SPS at 1300 °C.

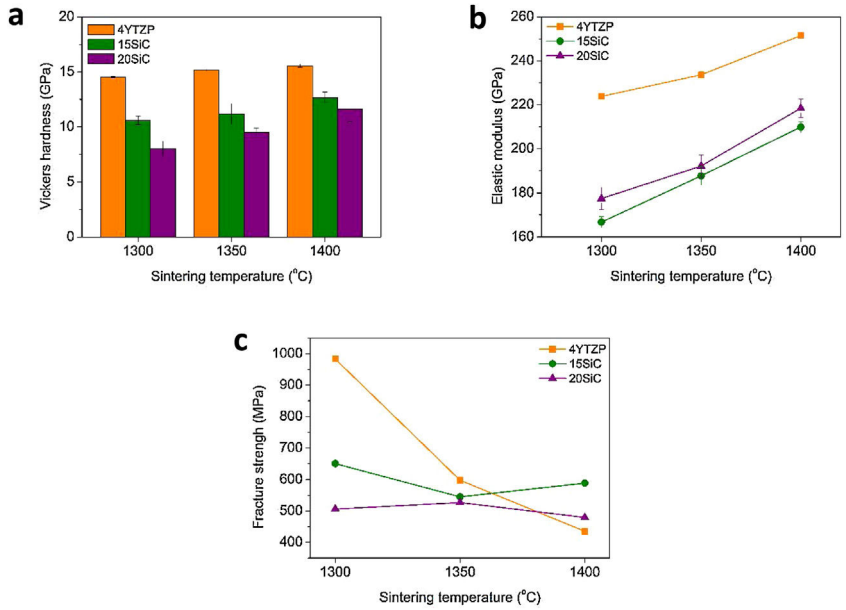

Fig. 8 – (a) Vickers hardness, (b) Young's modulus and (c) biaxial bending strength for 4YTZP and 4YTZP/SiC composites as a function of sintering temperature.

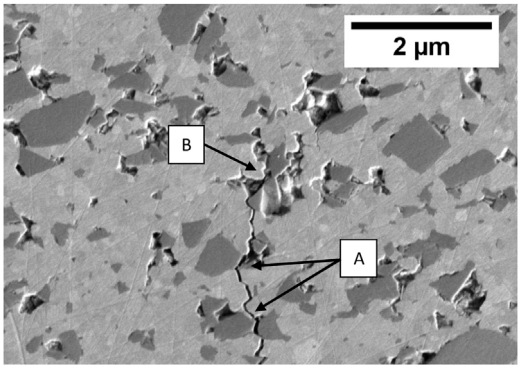

Fig. 9 – FE-SEM image of crack propagation of the 15SiC composite sintered at 1350 °C by SPS.

other according to expectation derived from the Hall–Petch law.

It can be observed that H_V in 4YTZP is similar at any sintering temperature (14.6–15.4 GPa). The highest hardness values for 15SiC and 20SiC composites were 12.7 GPa and 11.8 GPa, respectively, which were obtained at a sintering temperature of 1400 °C. At this temperature, SiC particles do not completely sinter, and sintering would have to be enhanced through higher temperatures or the use of additives. The authors had not found any hardness values for the ZrO_2–SiC composites sintered by spark plasma reported in the literature so far.

This behaviour could be explained by observing the microstructure of the sintered composites. As noted in the microstructure of the polished surface of the 15SiC composite sintered at 1350 °C (Fig. 9), certain defects arise during sintering due to the differences in the thermal expansion coefficient (around $4 \times 10^{-6}\,K^{-1}$ for SiC vs around $10 \times 10^{-6}\,K^{-1}$ for zirconia). This generates pores and removes grains, and these zones act as a stress absorption centre for the propagating cracks. Depending on its energy, the propagating crack can break SiC particles, as shown in Zone A in Fig. 9, or can be absorbed by the porous centres in Zone b [14,27].

Fig. 8c shows the relationship between the Young's modulus (*E*) and final temperature of different sintered materials. The minimum and maximum *E* values in each composite are shown by scatter bars. *E* values increase with sintering temperature in all cases, with this being higher in the case of 4YTZP material. The expected E value in 4YTZP/SiC composites would be higher than in 4YTZP; the main reason for this behaviour is the poor sinterability of SiC particles and the negative effect of porosity in the Young's modulus [28].

Fracture strength is shown in Fig. 8d. At the lowest temperature (1300 °C), the fracture strength of 4YTZP monolithic is very high, approaching 1000 MPa. At higher sintering temperatures, the fracture strength decreases to 600 and 450 MPa for 1350 and 1400 °C, respectively. At the lowest temperature (1300 °C), the strength of the composites is significantly lower than the 4YTZP material, but the composites show the highest strength at 1400 °C (~588 MPa and 492 MPa for 15SiC and 20SiC, respectively). The rationale for these trends is that the strength of brittle ceramics scales is inversely proportional with the square root of the dominant initial flaw size, where the size of that intrinsic flaw is expected to scale with the average grain the size.

In conclusion, mechanical properties are closely related to microstructure, which depends on grain size and porosity [29]. As shown in Fig. 7, the grain size of 4YTZP is ~114 nm at 1300 °C; for the 15SiC composite, the grain size of 4YTZP increases to ~143 nm, while it grows up to 322 mm for 20SiC composite. This increasing grain size with SiC percentage proves that SiC particles contribute to the grain growth of 4YTZP in composites, although they do not reach a full density (porosity ~5%), but improve the fracture strength.

Conclusion

Optimised suspensions of 4YTZP/SiC powders with 15 and 20 wt% SiC were obtained through colloidal processing and freeze-drying after the rheological behaviour of the aqueous suspensions of the starting powders. 4YTZP/SiC composites were successfully sintered by spark plasma at low temperatures (1300–1400 °C) without sintering aids. In order to determine the effect of SiC particles in a 4YTZP matrix, microstructure and mechanical properties of sintered composites were studied. Although SiC particles inhibit full densification, with final densities of 95–96% TD, they provoke an increase in the grain size of 4YTZP particles and their microstructure becomes less homogeneous. These microstructural features cause that the hardness and Young's modulus of the 4YTZP/SiC composites decrease with increasing SiC percentages due to their lower density. This means that 4YTZP/SiC composites are suitable for use in applications where high fracture strength is required.

Acknowledgements

The authors would like to thank the financial support received of the Spanish Ministry of Economy and Competitiveness (MINECO) under project MAT2015-67586-C3-R. A. Borrell acknowledge MINECO for RYC-2016-20915.

REFERENCES

[1] K. Houjou, K. Takahashi, K. Ando, Crack-healing behavior of ZrO_2/SiC composite ceramics and strength properties of crack-healing specimens, Int. J. Struct. Integr. 3 (2012) 41–52.
[2] K. Houjou, K. Ando, K. Takahashi, Crack-healing behaviour of ZrO_2/SiC composite ceramics, Int. J. Struct. Integr. 1 (2010) 73–84.
[3] S.K. Lee, Y.C. Kim, C.H. Kim, Microstructural development and mechanical properties of pressureless-sintered SiC with plate-like grains using Al_2O_3–Y_2O_3 additives, J. Mater. Sci. 29 (1994) 5321–5326.
[4] Z. He, H. Katsui, R. Tu, J. Zhang, T. Goto, High hardness and ductile mosaic SiC/SiO_2 composite by spark plasma sintering, J. Am. Ceram. Soc. 97 (2014) 681–683.
[5] D.G. Bekas, K. Tsirka, D. Baltzis, A.S. Paipetis, Self-healing materials: a review of advances in materials, evaluation, characterization and monitoring techniques, Compos. B Eng. 87 (2016) 92–119.
[6] Z. Derelioglu, S. Turteltaub, S. Van Der Zwaag, W.G. Sloof, Healing particles in self-healing thermal barrier coatings ICSHM, vol. 2013, 2013, pp. 578–581.
[7] N. Bamba, Y. Choa, T. Sekino, K. Niihara, Microstructure and mechanical properties of yttria stabilized zirconia/silicon carbide nanocomposites, J. Eur. Ceram. Soc. 18 (1998) 693–699.
[8] N. Bamba, Y.H. Choa, K. Niihara, Fabrication and mechanical properties of nanosized SiC particulate reinforced yttria stabilized zirconia composites, Nanostruct. Mater. 9 (1997) 497–500.
[9] N. Bamba, Y.H. Choa, T. Sekino, K. Niihara, Mechanical properties and microstructure for 3 mol% yttria doped zirconia/silicon carbide nanocomposites, J. Eur. Ceram. Soc. 23 (2003) 773–780.
[10] H.L. Lee, H.M. Lee, Effect of SiC on the mechanical properties of 3Y-TZP/SiC composites, J. Mater. Sci. Lett. 13 (1994) 974–976.
[11] R.M. Botella, Reología de suspensiones cerámicas, 2005.
[12] L. Gao, H.Z. Wang, J.S. Hong, H. Miyamoto, K. Miyamoto, Y. Nishikawa, S.D.D.L. Torre, SiC-ZrO_2(3Y)-Al_2O_3 nanocomposites superfast densified by Spark Plasma Sintering, Nanostruct. Mater. 11 (1999) 43–49.
[13] I. Álvarez-Clemares, A. Borrell, S. Agouram, R. Torrecillas, A. Fernández, Microstructure and mechanical effects of spark plasma sintering in alumina monolithic ceramics, Scr. Mater. 68 (2013) 603–606.
[14] O. García-Moreno, A. Borrell, B. Bittmann, A. Fernández, R. Torrecillas, Alumina reinforced eucryptite ceramics: very low thermal expansion material with improved mechanical properties, J. Eur. Ceram. Soc. 31 (2011) 1641–1648.
[15] L. Navarro, M.D. Salvador, A. Borrell, C.F. Gutiérrez-González, R. Moreno, Microestructura y propiedades mecánicas del composite SiC/Y-TZP/Al_2O_3 sinterizado por Spark Plasma Sintering, Material-ES 5 (2017) 87–90.
[16] J. Hong, L. Gao, S.D.D.L. Torre, H. Miyamoto, K. Miyamoto, Spark plasma sintering and mechanical properties of $ZrO_2(Y_2O_3)$–Al_2O_3 composites, Mater. Lett. 43 (2000) 27–31.
[17] V.M. Candelario, M.I. Nieto, F. Guiberteau, R. Moreno, A.L. Ortiz, Aqueous colloidal processing of SiC with $Y_3Al_5O_{12}$ liquid-phase sintering additives, J. Eur. Ceram. Soc. 33 (2013) 1685–1694.
[18] ASTM, C373-14 Standard Test Method for Water Absorption, Bulk Density, Apparent Porosity, and Apparent Specific Gravity of Fired Whiteware Products, (1999) Astm C373-88, vol. 88, Reapproved, p. 1–2.
[19] A.F. Kirstein, R.M. Woolley, Symmetrical bending of thin circular elastic plates on equally spaced point supports, J. Res. Natl. Bur. Stand. C Eng. Instrum. 71 (1966).
[20] F. Vitman, V. Pukh, A method for determining the strength of sheet glass, Ind. Lab. 29 (1963) 925–930.
[21] D.K. Shetty, A.R. Rosenfield, P. McGuire, G.K.W.H. Bansal, Duckworth: Biaxial Flexure Test for Ceramic Bulletin, vol. 59, 1980, pp. 1193–1197.
[22] V. Carnicer, C. Alcazar, E. Sánchez, R. Moreno, Aqueous suspension processing of multicomponent submicronic Y-TZP/Al_2O_3/SiC particles for suspension plasma spraying, J. Eur. Ceram. Soc. 38 (2018) 2430–2439.
[23] P. Carpio, R. Moreno, A. Gómez, M.D. Salvador, E. Sánchez, Role of suspension preparation in the spray drying process to obtain nano/submicrostructured YSZ powders for atmospheric plasma spraying, J. Eur. Ceram. Soc. 35 (2015) 237–247.
[24] R. Moreno, J.S. Moya, J. Requena, Electroquímica de suspensiones cerámicas, Bol. SECV 26 (1987) 355–365.
[25] S. Arcaro, A.P.N. Oliveira, C.F. Gutiérrez-Gonzalez, M.D. Salvador, A. Borrell, R. Moreno, LZS/Al_2O_3 nanostructured composites obtained by colloidal processing and spark plasma sintering, J. Eur. Ceram. Soc. 37 (2017) 5139–5148.
[26] S. Prochazka, R.M. Scalan, Effect of boron and carbon on sintering of SiC, J. Am. Ceram. Soc. 58 (1975) 72.
[27] G. Pezzotti, T. Nishida, M. Sakai, Physical limitations of the inherent toughness and strength in ceramic–ceramic and ceramic–metal nanocomposites, J. Ceram. Soc. Jpn. 103 (1995) 901–909.
[28] J. Luo, R. Stevens, Porosity-dependence of elastic moduli and hardness of 3Y-TZP ceramics, Ceram. Int. 25 (1999) 281–286.
[29] W.D. Kingery, Introduction to ceramics, J. Electrochem. Soc. 124 (1977) 152c.